Acta Oceanol. Sin., 2022, Vol. 41, No. 9, P. 107–116
https://doi.org/10.1007/s13131-022-2002-8
http://www.aosocean.com
E-mail: ocean2@hyxb.org.cn

Mounded seismic units in the modern canyon system in the Shenhu area, northern South China Sea: Sediment deformation, depositional structures or the mixed system?

Xishuang Li[1, 2*], Chengyi Zhang[1], Baohua Liu[3], Lejun Liu[1]

[1] First Institute of Oceanography, Ministry of Natural Resources, Qingdao 266061, China

[2] Laboratory for Marine Geology, Pilot National Laboratory for Marine Science and Technology (Qingdao), Qingdao 266237, China

[3] National Deep Sea Center, Ministry of Natural Resources, Qingdao 266237, China

Received 22 November 2020; accepted 5 February 2022

Abstract

The canyon system, including 17 small slope-confined canyons in the Shenhu area, northern South China Sea, is significantly characterized by mounded or undulating features on the canyon flanks and canyon heads. However, the mechanism underlying the formation of these features has yet to be elucidated. In previous studies, most of them were interpreted as sediment deformation on the exploration seismic profiles. In this paper, we collected high-resolution bathymetric data, chirp profiles and geotechnical test data to investigate their detailed morphology, internal structures, and origin. The bathymetric data indicated that most mounded seismic units have smooth seafloors and are separated by grooves or depressions. The distance between two adjacent mounded units is only hundreds of meters. On chirp profiles, mounded seismic units usually exhibit chaotic reflections and wavy reflections, of which the crests migrate upslope. The slope stability analysis results revealed that the critical angle of the soil layers in the study area tends to be 9°, indicating that most mounded seismic units on the canyon flanks and heads are stable at present. The terrain characteristics and seismic configurations combined with the slope stability analysis results indicated that most mounded seismic units are not sediment deformation but depositional structures or mixed systems composed of deformation and depositional structures.

Key words: northern South China Sea, submarine canyons, mounded seismic units, chirp profile, slope stability

Citation: Li Xishuang, Zhang Chengyi, Liu Baohua, Liu Lejun. 2022. Mounded seismic units in the modern canyon system in the Shenhu area, northern South China Sea: Sediment deformation, depositional structures or the mixed system?. Acta Oceanologica Sinica, 41(9): 107–116, doi: 10.1007/s13131-022-2002-8

1 Introduction

As one of the intensive sediment deformations, submarine landslides are widely distributed on continental margins worldwide and strongly shape marginal landforms and contribute to slope architecture (Bøe et al., 2000; Canals et al., 2004; Klaucke and Cochonat, 1999; Vanneste et al., 2006). Submarine landslides usually include a series of erosional and depositional processes that lead to a diversity of seismic signatures from chaotic sediment depocenters to well-stratified layers (O'Leary, 1991; Carlson et al., 1991; Hampton et al., 1996; Lee and Chough, 2001; Canals et al., 2004; Haflidason et al., 2004). Therefore, in many cases, it is difficult to distinguish between landslides and depositional structures, such as sediment waves and contourite drifts (Lee et al., 2002; Rebesco et al., 2009, 2014; Ribó et al., 2016). For example, the "Humboldt slide" on the Eel River continental margin in northern California was previously considered a slide (Gardner et al., 1999) and later considered as sedimentary waves caused by bottom currents (Lee et al., 2002). The origin of the seafloor wavy structures on the Adriatic shelf (Correggiari et al., 2001) and an extensive depositional body with nearly flat lying to slightly landward-dipping reflections in the Gulf of Alaska (Lee and Baraza, 1999) were once considered large landslides.

Seventeen small slope-confined canyons developed in the Shenhu area, north of the South China Sea (SCS), and cover water depths from ~300 m to ~2 000 m. These small canyons initiated in the middle Miocene (~13.8 Ma) and are characterized by periodic erosion-filling structures inside and thalweg migration eastward during their geological evolution (Zhu et al., 2010; Gong et al., 2013; Zhou et al., 2015; Jiang et al., 2017). Another significant phenomenon is that the seafloor in the canyon system is rough and rugged (Fig. 1), with complex topographic features (i.e., scarps, mounded units, depressions and grooves (Li et al., 2016)). Previous studies on the basis of exploration seismic data suggest that the undulated seafloor is mainly attributed to landslides or sediment creeps, which often exhibit mounded seismic units (He et al., 2014; Ma et al., 2015; Qiao et al., 2015). However, Li et al. (2019) grouped seafloor undulations, mounded seismic units with layer-ed reflections, into three types and considered undulations on canyon flanks as a result of sediment creeping and those on canyon heads and bottoms as a result of turbidity currents and internal waves. It is of great significance to clarify whether mounded units are sediment deformations or depos-

Foundation item: The National Natural Science Foundation of China under contract No. 41876061; the National Key Research and Development Program under contract No. 2016YFC0301403.
*Corresponding author, E-mail: lxs@fio.org.cn

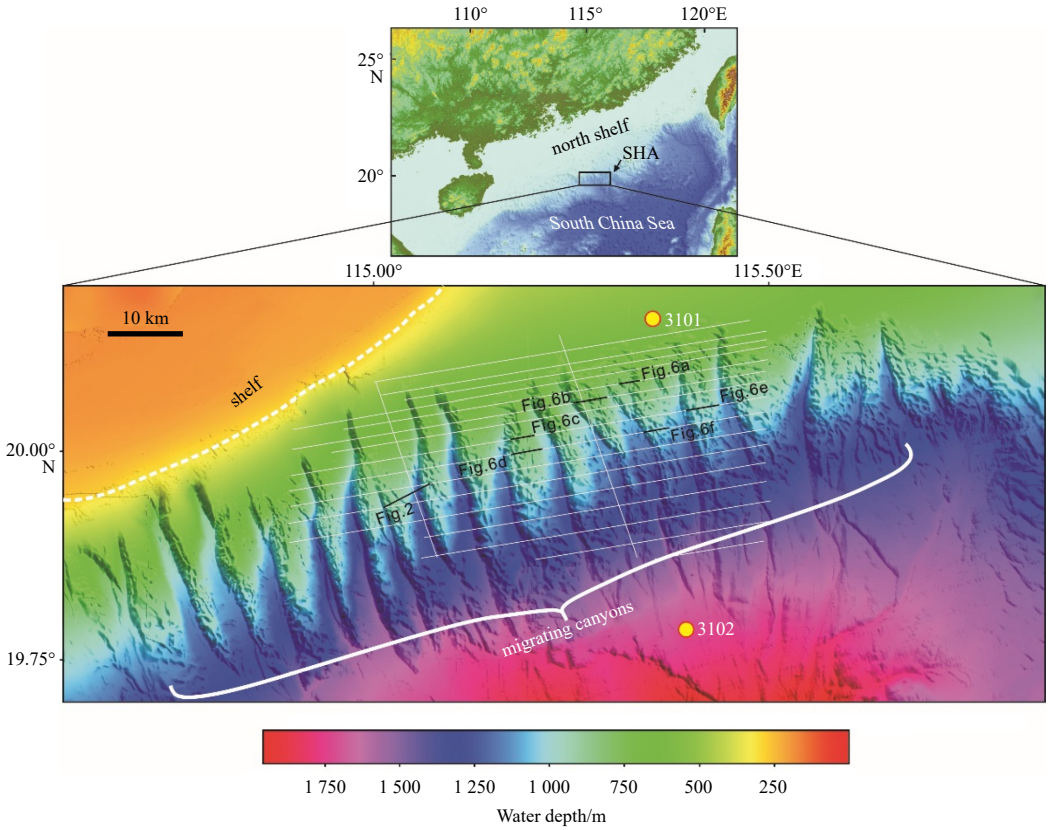

Fig. 1. Bathymetric map of the study area and geophysical data tracks. The study area is shown in the inserted map in the upper. The bathymetric map is based on multibeam bathymetric data combined with water depths derived from 3D seismic data. The shelf break is near the 250 m isobath. White thin lines represent subbottom profiles, and yellow dots denote 100-m boreholes. SHA: Shenhu area.

itional structures for understanding the geological evolution of the canyon system, geohazard assessment, and hydrocarbon exploration.

In this paper, the authors re-examined the physiographic characteristics and inner seismic architectures of mounded units on the basis of high-resolution geophysical data as well as the slope stability analysis results. The paper aims to (1) describe the detailed morphology and seismic configurations of mounded seismic units, (2) analyze the instability of mounded seismic units and (3) discuss the formation of these features.

2 Previous studies

2.1 *Geometry and distribution of landslides*

A few studies on submarine landslides in migrating canyon systems, mainly based on 2D/3D multichannel seismic (MCS) data, have been conducted in recent years (Qin, 2012; He et al., 2014; Qiao et al., 2015; Li et al., 2019). These studies documented the seismic morphology, size and geometric characteristics of accumulation systems and geomorphologic features associated with landslides (Fig. 2). He et al. (2014) described the geometry and distribution of the landslide in the canyon system:

(1) Landslides are grouped into three families: sediment creep, slump and landslide complex.

(2) Landslide area ranges from 0.53 km^2 to 18.09 km^2, with an average of 4.78 km^2 and less than 6 km^2 for 70% landslides.

(3) The depth of the landslide surface ranges from 40 m to 100 m.

(4) The travel distance of most landslide blocks is less than 3.5 km, with an average value of 1.89 km.

Zhou et al. (2019) also described the geometric characteristics and distribution of landslides using multibeam bathymetric data. More than 800 landslides were identified in the canyon area using a slope gradient method, and they show three basic planar shapes: round, belted-shaped and tongued shapes. The other geometric parameters (e.g., landslide area, thickness) obtained by the authors have similar results to those of He et al. (2014).

2.2 *Origin of sediment undulations*

Sediment undulations with well-layered configurations have been widely recognized on canyon heads, canyon flanks and bottoms in canyon systems (He et al., 2014; Qiao et al., 2015; Li et al., 2016; Li et al., 2019). For undulations developed on canyon heads and with crests parallel to the water isobaths, their origin is still controversial. He et al. (2014) and Qiao et al. (2015) suggested that they are sediment deformations caused by gravity, while Li et al. (2019) proposed that they may be caused by internal waves. There is also controversy about the origin of these sediment undulations on the canyon flanks. He et al. (2014) and Li et al. (2019) suggested that they are sediment creeping under gravitation, while Qiao et al. (2015) considered them the result of turbidity flows.

3 Data and methods

3.1 *Geophysical data*

The bathymetric data were collected with a shipborned EM302 SIMRAD^{TM} system operating at a frequency of 30 kHz in 2010, and a 40-m-resolution digital elevation model was gener-

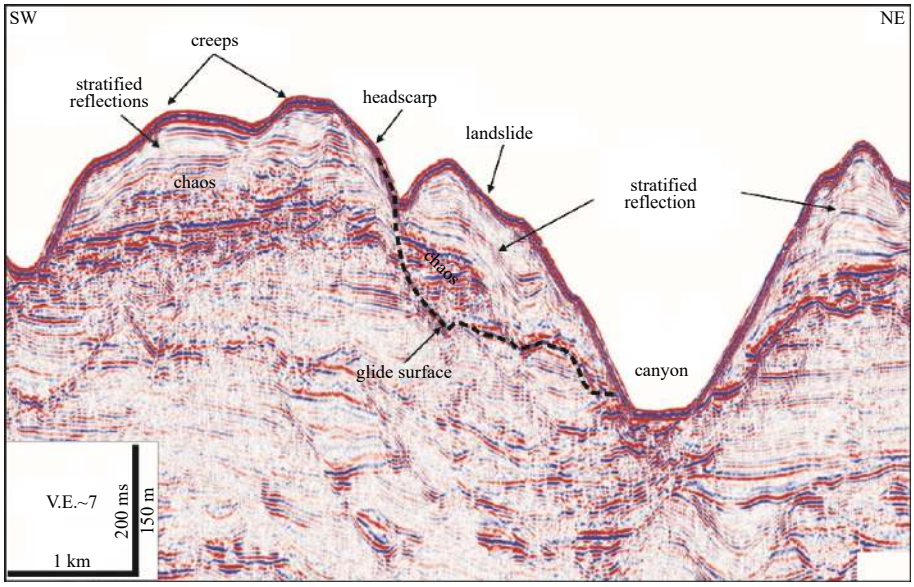

Fig. 2. Interpretation of landslides on an exploration seismic profile in the canyon flanks (after He et al., 2014). See Fig. 1 for the location. The seismic facies inside the landslides include chaotic and stratified reflections with variable amplitudes. V.E.~7 indicates that the vertical scale is exaggerated approximately 7 times.

ated by a combination of multibeam bathymetric data and bathymetric data derived from the 3D exploration seismic data. Slope gradients were calculated based on the bathymetric data using the software Surfer. Ultrahigh-resolution chirp profiles were collected synchronously using an IXSEA ECHOES 3500 system operating in chirp mode with sweep frequencies of 1.8–5.3 kHz and allowed us to observe more detailed internal structures of the mounded units than those shown on the exploration seismic profiles. The interpretation of acoustic facies refers to previous studies from O'Leary and Laine (1996), Hampton et al. (1996) and Lee et al. (2007).

3.2 *Geotechnical test data*

Geotechnical test data include the wet weight (kN/m^3) and undrained shear strength (kPa) of soil from two 100 m-long boreholes, which were drilled at water depths of 588 m (Borehole 3101) and 1 723 m (Borehole 3102) in 2013 (Fig. 1). The ring sampler method was used to measure the natural unit weight, and an electric vane shear tester was used to test the undrained shear strength.

A simple limit equilibrium method (Duncan, 1996) was used to calculate the safety factor and to discuss the relationship between the critical depth of the glide surface and its slope gradient angle. This method is usually used for predicting modern seafloor instability, not for landslides that have occurred, but it is suitable for sediment creeping, a very slow and usually ongoing sediment deformation. An infinite slope model was used, in which the stability of the slope is expressed by the safety factor (F_s). The F_s can be calculated by the following formula (Morgenstern and Price, 1965):

$$F_s = \{c+[(\gamma_w \times z+\gamma \times h)\times \cos 2\beta - u]\times \tan\varphi\}/(h\times\gamma'\times \sin\beta\times\cos\beta), \quad (1)$$

where c and u are cohesion and void pressure (kPa), respectively; γ, γ' and γ_w represent the bulk density of saturated soil, the density of soil in water and the density of water, respectively (kN/m^3); β and φ denote the slope angle and internal friction angle (°); z and h are water depth and sediment thickness (m); F_s is the safety factor, dimensionless. F_s equals to 1 suggests that the soil is in a critical state. When it is smaller than 1, the slope is in an unstable state and tends to fail; when it is greater than 1, the slope is in a stable state.

4 Results

4.1 *Morphological characteristics*

4.1.1 *Bathymetric data*

The seafloor in the study area is characterized by strong morphological variations, with a large variation in slope gradients (Fig. 3). The mounded terrain units are mainly found in the area with water depths ranging from ~600–1 400 m (Fig. 1). In the canyon heads and the upper area, the wavy terrain units are the remarkable topographic features perpendicular to the undercutting canyons. They extend along the along the contours, but they are not continuous because they are often broken off by the undercut canyons (Fig. 4a). The canyon flanks have large slope gradients and are dominated by elongated mounded or mounded terrain units and small grooves, as well as small depressions (Figs 4b, c). The adjacent canyons are separated by elongated mounded units that are usually parallel to the canyons. These elongated mounded units are not continuous from the canyon head to the tail but consist of intermittent segments, each of which is usually not more than 5 km in length. Large failure scars were also found on the canon flanks, and they are characterized by a downslope-opened semi-amphitheater-shaped or irregularly curved surface, referring to sediment transport events (Figs 5a–c). The headwall displays downslope-dipping steep surfaces with a slope gradient up to 10°.

Mounded terrain units often have smooth surfaces and are tens of meters high and hundreds of meters wide (Figs 5d–f). Their long axes are mainly parallel to the canyon axes, but some of them are perpendicular or oblique to the extension direction of the canyons. Shallow and gentle grooves with smooth surfaces, depths of 10–50 m and widths of hundreds of meters are often

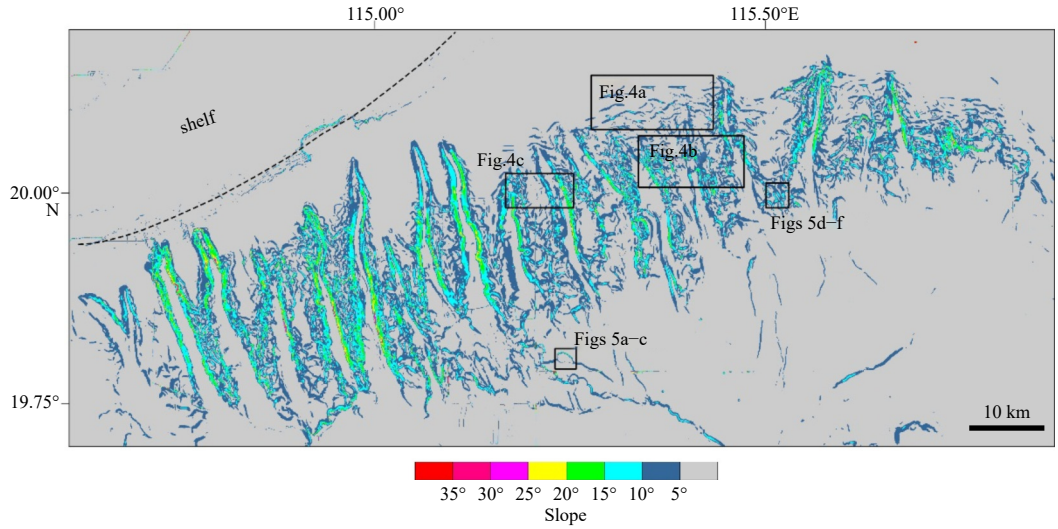

Fig. 3. Slope gradient map of the canyon area.

observed close to elongated mounds. The distance between the groove or the depression and the adjacent mounded unit is usually hundreds of meters (Figs 5d–f).

4.1.2 *Chirp profiles*

High-resolution chirp profiles allow us to distinguish two distinct seismic reflection configurations inside of the shallow unconsolidated sediments beneath the seabed: stratified reflections and chaotic reflections. Stratified reflections are characterized by medium to high seismic amplitudes and good lateral continuity, and they occur as parallel reflections and wavy reflections.

Deposit bodies are characterized by mounded or elongated mounded external shapes and were found on both sidewalls of the canyon. Their inner seismic configurations are mainly characterized by parallel or wavy reflections with good continuity and variable amplitudes (Fig. 6), and some of them are located on eroded surfaces (Figs 6a–e). Elongated or mounded deposit bodies on the canyon flanks and canyon heads mainly show parallel configurations or wavy reflections (Fig. 6), and they usually correspond to elongated or mounded terrain units on the bathymetric map. The stratified reflections of the elongated or mounded seismic units are often tens of meters thick and terminate at their margins by grooves, depressions or erosional surfaces (Figs 6a–e). In most cases, the crests of the wavy reflections inside elongated or mounded deposit bodies exhibit signs of moving upslope (Figs 6b, f). Chaotic or transparent/translucent reflections can be observed in the uppermost sediment layers, which are only a few meters thick and cover the older stratified layers (Figs 6a, b, d). The boundary between the young sediment layer and the older sediment layer is an erosional surface with high amplitude. The seafloor surfaces are usually characterized by seismic signatures of diffraction. Unfortunately, the distribution of chaotic reflections and stratified reflections cannot be determined by the current chirp survey lines.

4.2 *Slope stability analysis*

The shallow unconsolidated sediments in the canyon area are dominated by silty clay and clay (Jiang et al., 2018). Therefore, when taking the total stress as a parameter and without considering the effect of earthquake action, in Eq. (1), the internal friction angle (φ) equals zero, cohesion (c) equals the undrained shear strength (Su), and the stability or safety factor of the slope can be simplified as follows:

$$F_s = Su/(\sin\beta \times \cos\beta \times \gamma \times h). \tag{2}$$

For the parameter description in Eq. (2), see Eq. (1).

The sampling tests of two 100-m-long boreholes in the canyon area show that the wet bulk density of the soil at different depths does not change much and that the undrained shear strength basically increases linearly with depth (Fig. 7). In this paper, the wet bulk density is taken to be 16.5 kN/m^3, and the undrained shear strength can be described as follows:

$$Su = \text{sum} + k \times z, \tag{3}$$

where sum is the undrained shear strength of the topsoil and taken to 2.0 kPa; k represents the growth rate and is taken to 1.0 kPa/m; and z represents the depth of the soil. When only considering the gravity of the sediment itself and without considering external environmental factors such as earthquakes, the relationship between the sediment thickness (equivalent to the depth of the glide surface) and the slope gradient of the glide surface is shown in Fig. 8. The calculated result shows that as the depth of the glide surface increases, the critical angle of the soil layer tends to be 9° in the study area, which means that the soil layers will be stable when their slope gradient is less than 9° and only under their own weight.

5 Discussion

It is of great importance to understand the exact origin and formation processes of mounded seismic units, which are the dominant morphological features in canyon systems. Their significance is not only in geohazard assessments (Li et al., 2019) but also in the exploration of hydrocarbon resources in the Shenhu area (Gong et al., 2016). There is a large debate about the genesis of sediment undulations, which mainly display elongated and/or mounded seismic units in seismic profiles. Two hypotheses were proposed to explain the origin of the undulations in the study area: sediment formation, including landslides and sediment creeps, and depositional structures caused by turbidity currents and internal waves (He et al., 2014; Qiao et al., 2015; Li et al., 2019).

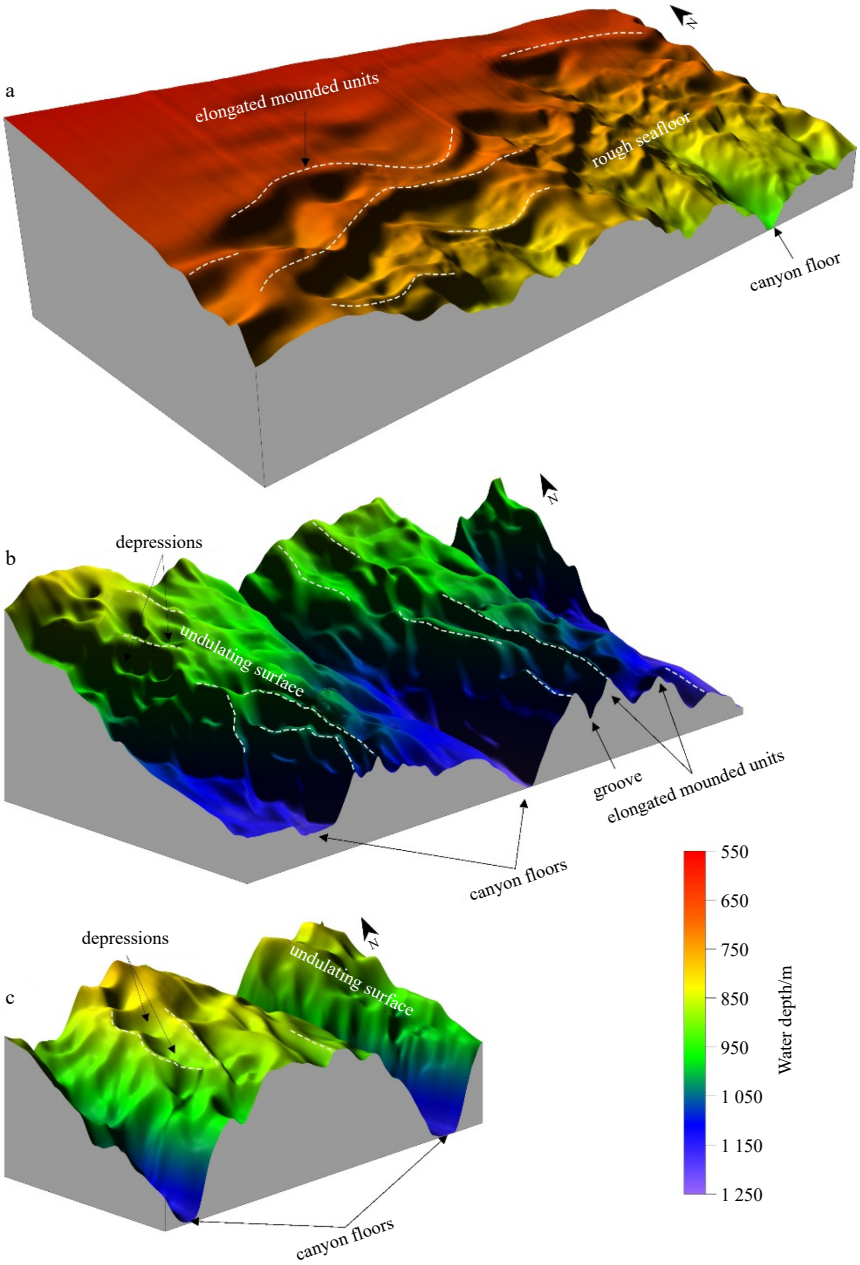

Fig. 4. 3D surface maps of canyon head (a) and canyon flanks (b, c). See Fig. 3 for their locations. White dotted lines represent splines of elongated mounded units.

Submarine landslides usually have an important impact on the seabed surface morphology (McAdoo et al., 2000; Baeten et al., 2013; Clare et al., 2018). In turn, the seabed morphologies and their changes are also effective signs for identifying submarine landslides. The eroded steep scar (slope gradient >15°) and associated seabed features with rough surfaces below the failure scars, such as hummocky deposits and eroded depressions, are usually indicators of submarine landslides, and the hummocky features are often interpreted as MTDs (Hampton et al., 1996; Clare et al., 2018). An average area of ~4.78 km^2 of landslides or collapses in the canyon system was reported by a previous study (He et al., 2014), which means that most landslides should be identified by bathymetric data with a spatial resolution of 40 m. This is not consistent with the morphological characteristics of the seabed surface impacted by landslides (Canals et al., 2004; Haflidason et al., 2004; Kukowski et al., 2008; Baeten et al., 2013). The multibeam bathymetric data show that the seafloor is undulating in the canyon flanks and canyon heads, but the seafloor surface is relatively smooth (Fig. 4), indicating that large landslide events might not occur frequently at present. Even if landslides occur, their size must be very small. Furthermore, if the elongated mounded units on the canyon flanks and canyon heads are landslides, it is difficult to imagine that the displaced sediments that are several kilometers long just moved a few hundred meters downslope.

Three types of submarine landslides were reported in the canyon system: sediment creeps, slumps and landslide complexes, and their thicknesses were estimated to be from 40 m to 100 m on the basis of exploration seismic data (He et al., 2014). However, high-resolution chirp profiles show that in shallow sed-

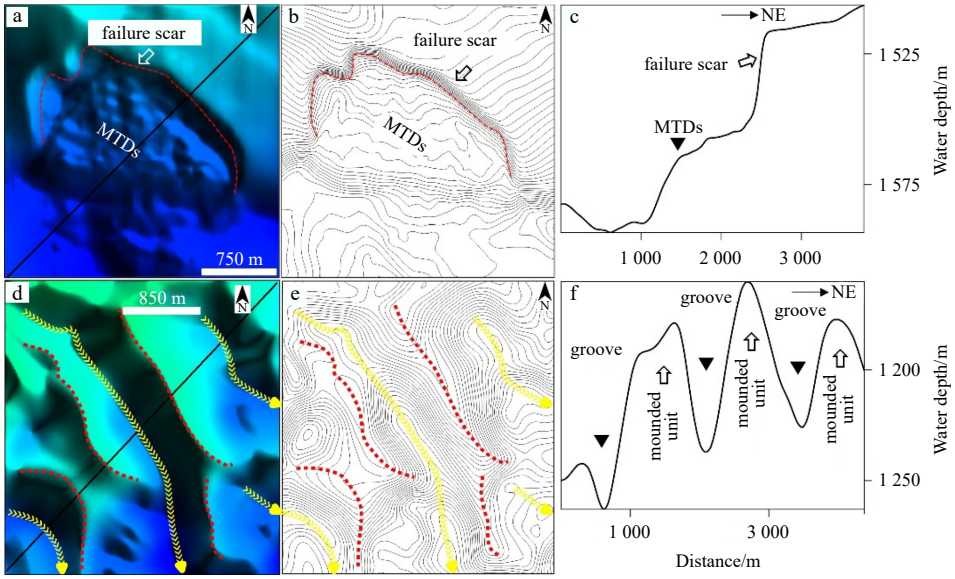

Fig. 5. Bathymetric map showing the morphology of a typical landslide (a–c) and the physiographic characterization of mounded seismic units on the canyon flank (d–f). See Fig. 3 for their locations. The red zigzag lines denote the failure scar of a slide, and the red dotted lines represent spines of mounded units. The yellow arrow lines represent grooves.

imentary layers beneath the sea floor, only small MTDs with chaotic facies are developed on canyon flanks, canyon bottoms and heads. These MTDs usually have a thickness of a few meters, lying on the older sediment layers with parallel or wavy reflections (Figs 6a–d). This is basically consistent with the size of the landslide observed on AUV-based chirp profiles (Liu et al., 2021). Most mounded seismic units are characterized by parallel or wavy internal reflections (Fig. 6), which suggests that they have not suffered from strong or rapid dynamic disturbance. Additionally, there are usually no distinct headwall scarps or zones of evacuation in the upslope direction of the mounded units (Fig. 6), both of which would typically be observed with traditional landslides (Hampton et al., 1996; Gee et al., 2006; Lee et al., 2002, 2007; Moscardelli and Wood, 2008; Bull et al., 2009; Chaytor et al., 2009; Berndt et al., 2012).

Mounded seismic units with stratified configurations on the canyon flanks were interpreted as sediment creeps that are related to gravitation (He et al., 2014; Qiao et al., 2015; Li et al., 2019). The “glide surfaces” at the bottoms of these mounded seismic units usually have a slope gradient less than 8° (He et al., 2014). The slope stability analysis results show that as the depth of the glide surface increases, the critical angle of the soil layer tends to 9°, which suggests that most “sediment creeps” might be stable at present. When considering seismic loads, as the seismic acceleration increases, the critical angle becomes significantly smaller (Zhou et al., 2019). However, from the perspective of the regional setting, seismic activity in the canyon area is weak (Sun et al., 2012), indicating that earthquakes are not the main triggering mechanism for landslides. Integrating the topographic characteristics and seismic configurations of mounded seismic units and the result of slope stability, we inferred that they might be depositional structures rather than sediment deformation.

A possible origin of these mounded seismic units on the canyon flanks and canyon heads is that they are related to internal waves or internal tides. In recent years, many studies have suggested that internal waves can lead to the generation of sediment waves (Karl et al., 1986; Masson et al., 2002; Reeder et al., 2011; Ribó et al., 2016). In the northern SCS, internal waves have been observed and reported (Li et al., 2011; Alford et al., 2015), and tides play a dominant role in driving internal tides and internal waves (Zhao et al., 2004; Li et al., 2008). In the canyon system, bottom current observations suggest that the alternating currents in the canyon are obvious, among which the internal tidal currents are dominant (Wu et al., 2016). Studies of the Baltimore (Gardner, 1989), Hudson (Hotchkiss and Wunsch, 1982) and Halibut canyons (Puig et al., 2013) show that internal waves/tides are responsible for the movement of particles in the canyon. We inferred the mounded seismic units with stratified reflections as the result of internal waves/tides, and the obvious surfaces at the bottoms of some mounded seismic units are not slide surfaces but erosional surfaces. The observed crest of wavy reflections migrating upslope supports our hypothesis.

Sediment complex bodies, which usually have a mounded external shape and a sandwich structure with alternating chaotic reflections and stratified configurations, might be mixed systems composed of deformation and depositional structures. The chaotic reflections indicate the destabilizing event of sediments, while the layered reflections indicate the deposition associated with the hydrodynamic environment. The bottom interfaces with slope gradients less than 9° below the complex bodies might be early erosion surfaces similar to the modern eroded seafloor.

6 Summary

High-resolution bathymetric data chirp profiles allowed us to describe the detailed morphology and internal configurations of widespread mounded units and to discuss their origin together with an analysis of slope stability. The main conclusions of this work are as follows:

(1) The mounded seismic units exhibit two typical seismic facies: chaotic reflections and stratified reflections. Most of them have smooth seafloor and are tens of meters high, hundreds of meters wide and separated by grooves or depressions. The distance between two adjacent mounded units is only hundreds of meters.

(2) The slope stability analysis results show that the critical angle of the soil layers in the study area tends to be 9°, indicating

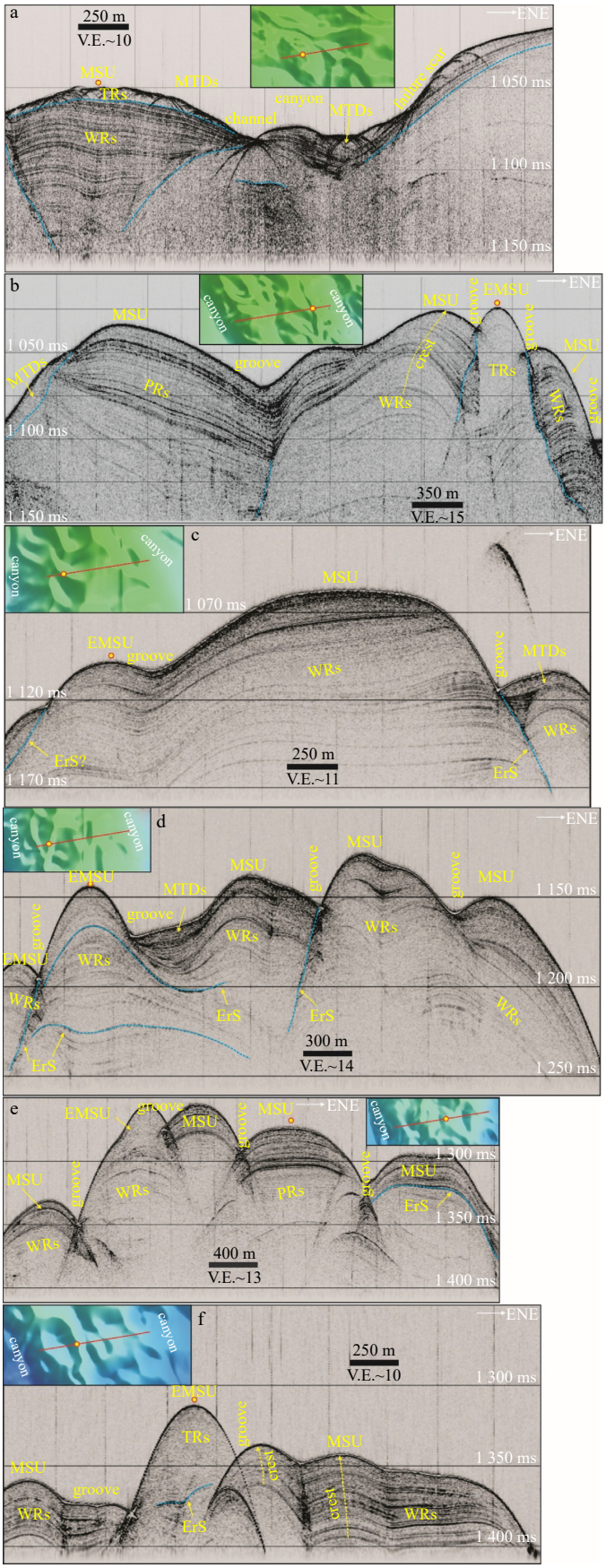

Fig. 6. Chirp profiles show seismic architectures of elongated or mounded units on the canyon flanks. See Fig. 1 for their tracks. WRs: wavy reflections; TRs: translucent reflections; PRs: parallel reflections; ErS: electronic surface; MSU: mounded seismic units; EMSU: elongated mounded seismic units. Blue dotted lines denote erosional surfaces. V.E.~10 indicates that the vertical scale is exaggerated approximately 10 times.

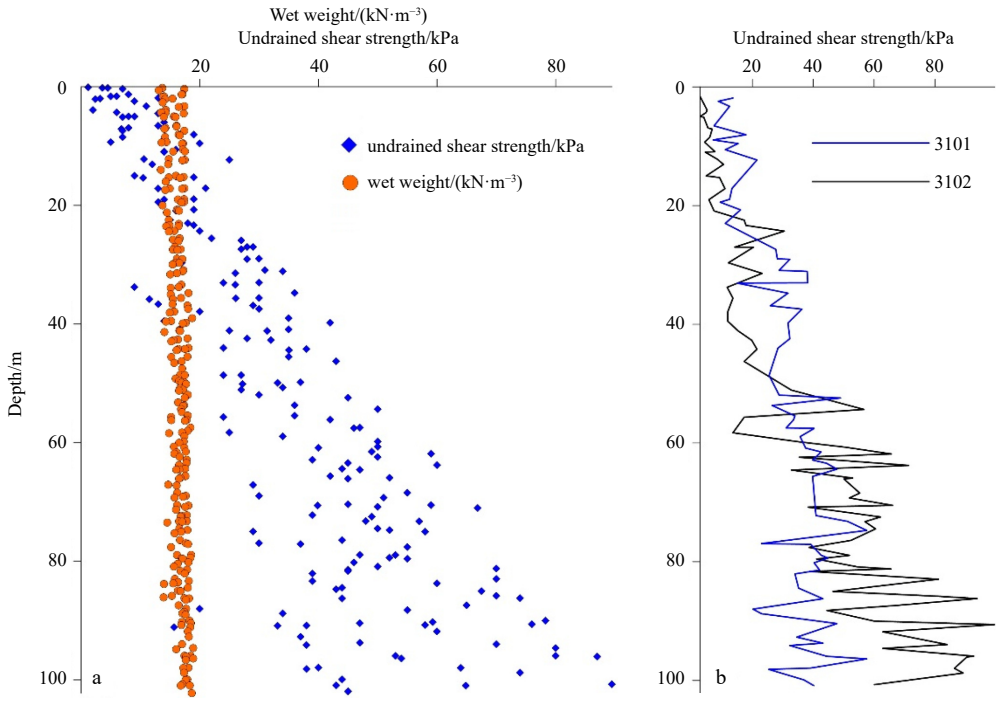

Fig. 7. Variation in wet bulk density and undrained shear strength vs. depth in two 100-m boreholes (a) and undrained shear strength profiles at Boreholes 3101 and 3102 (b). The locations of the boreholes are shown in Fig. 1.

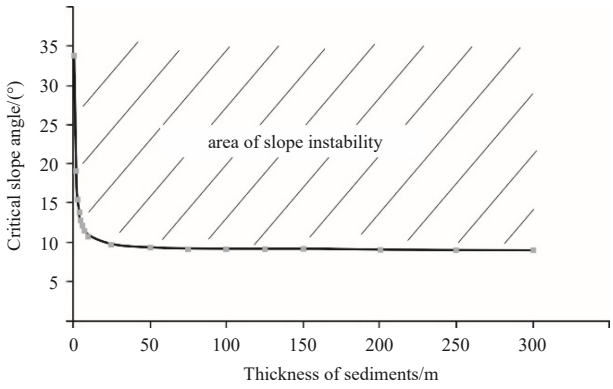

Fig. 8. Critical angle of the slope vs. the depth of the glide surface. The area above the black solid curve represents the insatiability zone for sediments on the slope. In the canyon system, the critical angle of the landslides is ~9°.

that most mounded seismic units on canon flanks and heads are stable.

(3) The mounded seismic units were overinterpreted as sediment deformation, possibly due to the canyon environment. Some of them are landslides, but most of them are depositional structures caused by ocean dynamic environments. The landslide complexes proposed in previous studies might be mixed systems composed of deformation and depositional structures. Additional detailed investigations, such as bottom current observations and sediment fluxes, are needed.

Acknowledgements

We are deeply grateful for the exchange of ideas with Sebastian Krastel, and we thank the technical staff and crew in the field work. We are also grateful to the three reviewers and their constructive comments that improved the quality of the manuscript.

References

Alford M H, Peacock T, MacKinnon J A, et al. 2015. The formation and fate of internal waves in the South China Sea. Nature, 521(7550): 65–69, doi: 10.1038/nature14399

Baeten N J, Laberg J S, Forwick M, et al. 2013. Morphology and origin of smaller-scale mass movements on the continental slope off northern Norway. Geomorphology, 187: 122–134, doi: 10.1016/j.geomorph.2013.01.008

Berndt C, Costa S, Canals M, et al. 2012. Repeated slope failure linked to fluid migration: the Ana submarine landslide complex, Eivissa Channel, western Mediterranean Sea. Earth and Planetary Science Letters, 319–320: 65–74

Bøe R, Hovland M, Instanes A, et al. 2000. Submarine slide scars and mass movements in Karmsundet and Skudenesfjorden, southwestern Norway: morphology and evolution. Marine Geology, 167(1–2): 147–165, doi: 10.1016/S0025-3227(00)00017-7

Bull S, Cartwright J, Huuse M. 2009. A review of kinematic indicators from mass-transport complexes using 3D seismic data. Marine and Petroleum Geology, 26(7): 1132–1151, doi: 10.1016/j.marpetgeo.2008.09.011

Canals M, Lastras G, Urgeles R, et al. 2004. Slope failure dynamics and impacts from seafloor and shallow sub- seafloor geophysical data: case studies from the COSTA project. Marine Geology, 213(1–4): 9–72, doi: 10.1016/j.margeo.2004.10.001

Carlson P R, Karl H A, Edwards B D. 1991. Mass sediment failure and transport features revealed by acoustic techniques, Beringian margin, Bering Sea, Alaska. Marine Geotechnology, 10(1–2): 33–51, doi: 10.1080/10641199109379881

Chaytor J D, ten Brink U S, Solow A R, et al. 2009. Size distribution of submarine landslides along the U.S. Atlantic margin. Marine Geology, 264(1–2): 16–27, doi: 10.1016/j.margeo.2008.08.007

Clare M, Chaytor J, Dabson O, et al. 2018. A consistent global approach for morphometric characterisation of subaqueous landslides. In: Lintern D G, Mosher D C, Moscardelli L G, et al., eds. Subaqueous Mass Movements. London: Geological Society, Special Publications, 455–477

Correggiari A, Trincardi F, Langone L, et al. 2001. Styles of failure in

late Holocene highstand prodelta wedges on the Adriatic shelf. Journal of Sedimentary Research, 71(2): 218–236, doi: 10.1306/042800710218
Duncan J M. 1996. State of the art: limit equilibrium and finite-element analysis of slopes. Journal of Geotechnical Engineering, 122(7): 577–596, doi: 10.1061/(ASCE)0733-9410(1996)122:7(577)
Gardner W D. 1989. Baltimore Canyon as a modern conduit of sediment to the deep sea. Deep-Sea Research Part A. Oceanographic Research Papers, 36(3): 323–358
Gardner J V, Prior D B, Field M E. 1999. Humboldt slide — a large shear-dominated retrogressive slope failure. Marine Geology, 154(1–4): 323–338, doi: 10.1016/S0025-3227(98)00121-2
Gee M J R, Gawthorpe R L, Friedmann S J. 2006. Triggering and evolution of a giant submarine landslide, offshore Angola, revealed by 3D seismic stratigraphy and geomorphology. Journal of Sedimentary Research, 76(1): 9–19, doi: 10.2110/jsr.2006.02
Gong Chenglin, Wang Yingmin, Zhu Weilin, et al. 2013. Upper Miocene to Quaternary unidirectionally migrating deep-water channels in the Pearl River Mouth Basin, northern South China Sea. AAPG Bulletin, 97(2): 285–308, doi: 10.1306/07121211159
Gong Chenglin, Wang Yingmin, Zheng Rongcai, et al. 2016. Middle Miocene reworked turbidites in the Baiyun Sag of the Pearl River Mouth Basin, northern South China Sea margin: processes, genesis, and implications. Journal of Asian Earth Sciences, 128: 116–129, doi: 10.1016/j.jseaes.2016.06.025
Haflidason H, Sejrup H P, Nygård A, et al. 2004. The Storegga Slide: architecture, geometry and slide development. Marine Geology, 213(1–4): 201–234, doi: 10.1016/j.margeo.2004.10.007
Hampton M A, Lee H J, Locat J. 1996. Submarine landslides. Reviews of Geophysics, 34(1): 33–59, doi: 10.1029/95RG03287
He Ye, Zhong Guangfa, Wang Liaoliang, et al. 2014. Characteristics and occurrence of submarine canyon-associated landslides in the middle of the northern continental slope, South China Sea. Marine and Petroleum Geology, 57: 546–560, doi: 10.1016/j.marpetgeo.2014.07.003
Hotchkiss F S, Wunsch C. 1982. Internal waves in Hudson Canyon with possible geological implications. Deep-Sea Research Part A. Oceanographic Research Papers, 29(4): 415–442
Jiang Jing, Shi Hesheng, Lin Changsong, et al. 2017. Sequence architecture and depositional evolution of the Late Miocene to quaternary northeastern shelf margin of the South China Sea. Marine and Petroleum Geology, 81: 79–97, doi: 10.1016/j.marpetgeo.2016.12.025
Jiang Heng, Su Ming, Lei Xinhua, et al. 2018. Distribution of fine-grained turbidites on canyon ridges in the Shenhu area of northern South China Sea and its implications. Marine Geology & Quaternary Geology, 38(5): 52–62
Karl H A, Cacchione D A, Carlson P R. 1986. Internal-wave currents as a mechanism to account for large sand waves in Navarinsky Canyon head, Bering Sea. Journal of Sedimentary Research, 56(5): 706–714
Klaucke I, Cochonat P. 1999. Analysis of past sea floor failures on the continental slope off Nice (SE France). Geo-Marine Letter, 19: 245–253
Kukowski N, Hampel A, Hoth S, et al. 2008. Morphotectonic and morphometric analysis of the Nazca plate and the adjacent offshore Peruvian continental slope—Implications for submarine landscape evolution. Marine Geology, 254(1–2): 107–120, doi: 10.1016/j.margeo.2008.05.017
Lee H, Baraza J. 1999. Geotechnical characteristics and slope stability in the Gulf of Cadiz. Marine Geology, 155(1–2): 173–190, doi: 10.1016/S0025-3227(98)00146-7
Lee S H, Chough S K. 2001. High-resolution (2–7 kHz) acoustic and geometric characters of submarine creep deposits in the South Korea Plateau, East Sea. Sedimentology, 48(3): 629–644, doi: 10.1046/j.1365-3091.2001.00383.x
Lee H J, Locat J, Desgagnés P, et al. 2007. Submarine mass movements on continental margins. In: Nittrouer C A, Austin J A, Field M E, eds. Continental Margin Sedimentation: From Sediment Transport to Sequence Stratigraphy. Malden: Blackwell Publishing, 213–274
Lee H J, Syvitski J P M, Parker G, et al, 2002. Distinguishing sediment waves from slope failure deposits: field examples, including the 'humboldt slide', and modelling results. Marine Geology, 192(1–3): 79–104
Li D, Chen X, Liu A. 2011. On the generation and evolution of internal solitary waves in the northwestern South China Sea. Ocean Modelling, 40(2): 105–119, doi: 10.1016/j.ocemod.2011.08.005
Li Jian, Li Wei, Alves T M, et al. 2019. Different origins of seafloor undulations in a submarine canyon system, northern South China Sea, based on their seismic character and relative location. Marine Geology, 413: 99–111, doi: 10.1016/j.margeo.2019.04.007
Li Xiaofeng, Zhao Zhongxiang, Pichel W G. 2008. Internal solitary waves in the northwestern South China Sea inferred from satellite images. Geophysical Research Letters, 35(13): L13605, doi: 10.1029/2008GL034272
Li Xishuang, Zhou Qingjie, Su Tianyun, et al. 2016. Slope-confined submarine canyons in the Baiyun deep-water area, northern South China Sea: variation in their modern morphology. Marine Geophysical Research, 37(2): 95–112, doi: 10.1007/s11001-016-9269-0
Liu Zheng, Chen Duanxin, Zhu Yousheng, et al. 2021. Geophysical studies of mass transport deposits on the slope canyon floor with high-resolution autonomous underwater vehicle (AUV) in the Shenhu area and its implications for sediment transportation. Marine Geology & Quaternary Geology, 41(2): 13–21
Ma Benjun, Wu Shiguo, Sun Qiliang, et al. 2015. The late Cenozoic deep-water channel system in the Baiyun Sag, Pearl River Mouth Basin: development and tectonic effects. Deep-Sea Research Part II: Topical Studies in Oceanography, 122: 226–239, doi: 10.1016/j.dsr2.2015.06.015
Masson D G, Howe J A, Stoker M S. 2002. Bottom-current sediment waves, sediment drifts and contourites in the northern Rockall Trough. Marine Geology, 192(1–3): 215–237, doi: 10.1016/S0025-3227(02)00556-X
McAdoo B G, Pratson L F, Orange D L. 2000. Submarine landslide geomorphology, US continental slope. Marine Geology, 169(1–2): 103–136, doi: 10.1016/S0025-3227(00)00050-5
Morgenstern N R, Price V E. 1965. The analysis of the stability of general slip surfaces. Géotechnique, 15(1): 79–93
Moscardelli L, Wood L. 2008. New classification system for mass transport complexes in offshore Trinidad. Basin Research, 20(1): 73–98, doi: 10.1111/j.1365-2117.2007.00340.x
O'Leary D W. 1991. Structure and morphology of submarine slab slides: Clues to origin and behavior. Marine Geouchnology, 10: 53–69, doi: 10.1080/10641199109379882
O'Leary D W, Laine E. 1996. Proposed criteria for recognizing intrastratal deformation features in marine high resolution seismic reflection profiles. Geo-Marine Letters, 16(4): 305–312, doi: 10.1007/BF01245561
Puig P, Greenan B J W, Li M Z, et al. 2013. Sediment transport processes at the head of Halibut Canyon, eastern Canada margin: an interplay between internal tides and dense shelf-water cascading. Marine Geology, 341: 14–28, doi: 10.1016/j.margeo.2013.05.004
Qiao Shaohua, Su Ming, Kuang Zenggui, et al. 2015. Canyon-related undulation structures in the Shenhu area, northern South China Sea. Marine Geophysical Research, 36(2): 243–252
Qin Zhiliang. 2012. Sedimentary process, distribution and mechanism of mass transport deposits, the slope area of northern South China Sea (in Chinese)[dissertation]. Qingdao: Institute of Oceanology, Chinese Academy of Sciences
Rebesco M, Hernández-Molina F J, Van Rooij D, et al. 2014. Contourites and associated sediments controlled by deep-water circulation processes: state-of-the-art and future considerations. Marine Geology, 352: 111–154, doi: 10.1016/j.margeo.2014.03.011
Rebesco M, Neagu R C, Cuppari A, et al. 2009. Morphobathymetric analysis and evidence of submarine mass movements in the western Gulf of Taranto (Calabria margin, Ionian Sea). International Journal of Earth Sciences, 98(4): 791–805, doi:

10.1007/s00531-009-0429-1

Reeder D B, Ma B B, Yang Y J. 2011. Very large subaqueous sand dunes on the upper continental slope in the South China Sea generated by episodic, shoaling deep-water internal solitary waves. Marine Geology, 279(1–4): 12–18, doi: 10.1016/j.margeo.2010.10.009

Ribó M, Puig P, Muñoz A, et al. 2016. Morphobathymetric analysis of the large fine-grained sediment waves over the Gulf of Valencia continental slope (NW Mediterranean). Geomorphology, 253: 22–37, doi: 10.1016/j.geomorph.2015.09.027

Sun Jinlong, Xu Huilong, Zhan Wenhuan, et al. 2012. Activity and triggering mechanism of seismic belt along the northern South China Sea continental margin. Journal of Tropical Oceanography, 31(3): 40–47

Vanneste M, Mienert J, Bünz S. 2006. The Hinlopen Slide: a giant, submarine slope failure on the northern Svalbard margin, Arctic Ocean. Earth and Planetary Science Letters, 245(1–2): 373–388, doi: 10.1016/j.epsl.2006.02.045

Wu Lunyu, Xiong Xuejun, Li Xiaolong, et al. 2016. Bottom currents observed in and around a submarine valley on the continental slope of the northern South China Sea. Journal of Ocean University of China, 15(6): 947–957, doi: 10.1007/s11802-016-3054-1

Zhao Zhongxiang, Klemas V, Zheng Quanan, et al. 2004. Remote sensing evidence for baroclinic tide origin of internal solitary waves in the northeastern South China Sea. Geophysical Research Letters, 31(6): L06302

Zhou Qingjie, Li Xishuang, Zhou Hang, et al. 2019. Characteristics and genetic analysis of submarine landslides in the northern slope of the South China Sea. Marine Geophysical Research, 40(3): 303–314, doi: 10.1007/s11001-018-9369-0

Zhou Wei, Wang Yingmin, Gao Xianzhi, et al. 2015. Architecture, evolution history and controlling factors of the Baiyun submarine canyon system from the middle Miocene to Quaternary in the Pearl River Mouth Basin, northern South China Sea. Marine and Petroleum Geology, 67: 389–407, doi: 10.1016/j.marpetgeo.2015.05.015

Zhu Mangzheng, Graham S, Pang Xiong, et al. 2010. Characteristics of migrating submarine canyons from the middle Miocene to present: implications for paleoceanographic circulation, northern South China Sea. Marine and Petroleum Geology, 27(1): 307–319, doi: 10.1016/j.marpetgeo.2009.05.005